

THE EFFECT OF FOLDING ON THE INTERNAL STRUCTURE OF BALLISTIC FIBERS

*Haruki Kobayashi^a, Walter G. McDonough^a, Hae-Jeong Lee^a, Jae Hyun Kim^a,
Amanda L. Forster^b, Kirk D. Rice^b, Gale A. Holmes^a*

*National Institute of Standards and Technology
^aPolymers Division, ^bOffice of Law Enforcement Standards
100 Bureau Drive
Gaithersburg, Maryland 20899*

ABSTRACT

In a previous study, the mechanical properties of poly (*p*-phenylene benzobisoxazole) (PBO) fibers were degraded when the fibers were folded. When poly (*p*-phenylene terephthalamide) (PPTA) fibers were examined, a similar drop in mechanical properties was not observed. In the present study, the possibility of structural changes in PBO and PPTA fibers caused by folding were investigated by using small angle X-ray scattering (SAXS). From these findings, one may postulate that the fibrils in the PBO fibers were subdivided when the fibers were folded whereas the PPTA fibers did not appear to change. The subdivision for PBO fibers may create new surfaces and defects inside the fibers. Thus, the subdivision may influence not only mechanical properties, but also hydrolytic degradation and other failure pathways.

1. INTRODUCTION

In recent years, researchers at the National Institute of Standards and Technology (NIST) investigated the reasons why a vest was perforated in the field by a threat that it was rated to withstand.¹ In addition, NIST was charged with developing evaluation methods that quantify improvements in the next generation of fibers that may be used in soft body armor (SBA), with a special focus on their long-term performance.¹⁻³ To date, the focus has been on poly (*p*-phenylene benzobisoxazole) (PBO) fibers and poly (*p*-phenylene terephthalamide) (PPTA) fibers.

The first step in this study was to characterize the chemical and physical properties of the PBO fibers that had been extracted from the field-perforated body armor.⁴ Because of the conditions under which the SBA was used, an initial hypothesis was that hydrolytic degradation of the PBO fibers was the source of the failure. To further investigate this hypothesis, ballistic tests were conducted on a SBA that was hydrolytically aged in the laboratory such that yarns extracted from this SBA showed a comparable decrease in mechanical properties to the mechanical properties measured from yarns taken from the back panel of the field-perforated body armor (the front panel was unavailable). Although the mechanical properties were reduced to a comparable level, no threat level projectiles passed through the vests. This result raised three questions:

1. Is there a correlation between mechanical properties as measured on fibers and yarns and the ballistic performance of SBA?
2. Are the mechanical properties of the back panel of the field-perforated armor the same as the mechanical properties of the front panel?
3. Could there be other degradation methods that may have an effect on armor durability?

The first question addresses the ability to establish a correlation between mechanical property tests that are performed at slow rates with ballistic performance tests. This question will be addressed in future work. To address the second question, one can imagine that the front panel of a bullet resistant vest experiences more mechanical stress from folding and thus the fabric in the front panel could deteriorate at a faster rate. If this is the case, then one could expect a non-uniform deterioration in fiber properties and should not be surprised that the conditioned SBAs passed the ballistic performance test, since their level of deterioration were targeted from the properties of the back panel. For the third question, folding the fabric in the vest could cause degradation and could combine synergistically with other degradation routes. Folding, especially in the front panel, would be a natural event, especially in thinner or more flexible SBAs.

One of the main differences between PBO fibers and PPTA fibers seems to stem from microstructural characteristics. PPTA has extensive hydrogen bonding between chains whereas PBO fibers do not have such bonds.⁵ To address the third question in more detail, the work of Kitagawa et al. was considered, wherein they conducted an extensive study of the morphology of PBO fibers.⁶ They used small angle X-ray scattering (SAXS), wide angle X-ray diffraction, dark-field images of transmission electron microscopy (TEM) and scanning electron microscopy (SEM). This work identified sharp diffraction spots along the equator and “streak-like” layer lines. Additionally, they proposed a structural model for PBO that contained microfibrils and microvoids in the center part of the fiber and a void-free section on the surface estimated to have a thickness of 0.2 μm .

As the proposed structure of PBO is considered, along with the environmental factors that SBA typically encounters, one may postulate that folding may be a cause of the reduction in mechanical properties that had been observed in vests comprised of PBO fibers.⁷ A device was built to repeatedly fold fabric taken from armor in an effort to mimic the type of folding seen in the field. After folding the fibers 80 000 times, a reduction in the tensile strength of the fibers of 41 % was measured. Using SAXS, changes in the microstructure of the fibers after folding were detected. Furthermore, failure analysis using SEM on tested fibers revealed changes in failure morphology (see Figure 1). In these SEM images, the fibrils in the fracture surface of the unfolded PBO were thicker and longer than the fibrils in the fracture surface of 80 000 folded PBO. In the single fold test, kink bands were observed in PBO and PPTA fibers by using optical microscopy.⁸ However, in the 80 000 fold test, no kink bands could be observed with an optical microscope. With the single fold test, the radius of curvature was about 0.05 mm. Thus, the kink bands that had been observed by single fold test may have been a result of a severe radius of curvature. Chau et al. observed similar kink band formation in PBO fibers when they folded single fibers around a 1.27 mm pin.⁹ In the 5 000 and 80 000 fold tests, the radius of curvature was 3.15 mm.

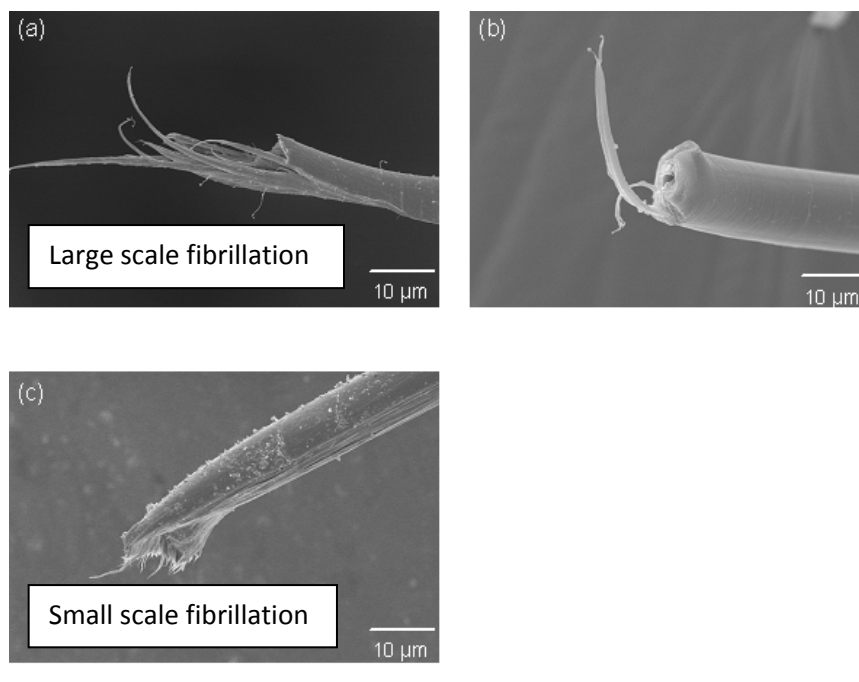


Figure 1. Fracture surface of the (a) unfolded, (b) 5 500, and (c) 80 000 PBO fibers.

This paper documents the quantification of properties of folded PBO and PPTA fibers using the single fiber test and their subsequent interrogation using the SAXS technique. For the SAXS work, untensioned yarns of PBO fibers were interrogated by an X-ray beam to observe possible internal damage. The methodology used to quantify the data is taken from Shioya and Takaku¹⁰ who developed an approach to characterize voids in carbon fibers using SAXS. The SAXS analysis based on the law of Guinier is a practical method to obtain the information of the microvoids in materials. Shioya and Takaku developed a method to analyze SAXS from voids in a unidirectionally aligned fibrous material, and this method was used to analyze the structural changes caused by folding tests.

2. EXPERIMENTAL

Single factor analysis of variance (ANOVA) was performed on the data to determine if there were significant statistical variations among the data sets. Each data set consisted of 50 single fiber tests. The reported standard deviations are taken as an estimate of the standard uncertainties of the measurements.

2.1 Fiber Folding

The folding apparatus used in these experiments was described previously.⁷ Figure 2A shows the folding apparatus containing a layer of fabric that was extracted from a vest and folded around a 6.3 mm diameter bar. This bar is designed to be representative of a reasonable folding angle for SBA. As seen in Figure 2B, the frame is opened and closed to mimic folding that a SBA may experience. Note that constant force springs are used to ensure that the fabric is not placed under high tension during the folding process.

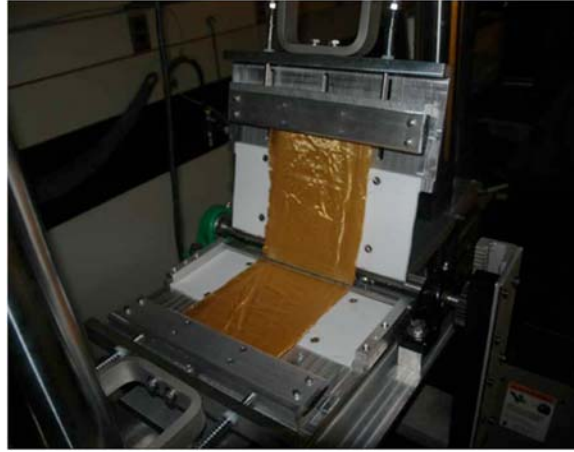


Figure 2A. Folding device with fabric clamped in the sliding brackets and around the folding rod.⁸ (Used with permission by ASME).

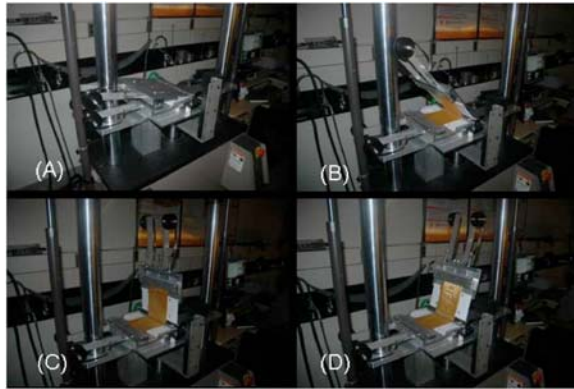


Figure 2B. Collage showing the fabric as it goes from the closed position, A, to the fully open position, D.⁸ (Used with permission by ASME).

2.2 Single Fiber Test

The technique used to conduct the single fiber tests was discussed in detail previously.¹¹ Briefly, yarns were removed from the fabric, and then single fibers were removed from the yarns then bonded to paper templates that had a gage length of 60 mm. The strain measurements were made with a laser extensometer, as this allowed for direct measurement of strain. This gauge length was selected because the instrument requires a minimum gauge length of 51 mm for optimal performance. Fiber diameters were measured at 5 different locations along the fiber. The testing speed was 2 mm/min.

2.3 SAXS

The specimens for the SAXS measurements were prepared by stretching fiber yarns axially across two paper tabs as shown in Figure 3. The fiber yarns were bonded to paper tabs using an adhesive that cured at room temperature overnight, and care was taken not to let the glue diffuse into the area of the beam. The SAXS measurements were conducted by using pinhole collimated

$\text{CuK}\alpha$ radiation as the incident beam (Figure 4). Two-dimensional images of SAXS were taken with an imaging plate. The sample-to-detector distances (SDDs) were 3426 mm for SAXS measurement of PPTA fiber, and 4060 mm for SAXS measurement of PBO fibers, with the SDDs chosen to optimize the measurement. The X-ray beam irradiated the fiber specimen perpendicular to the fiber axis.

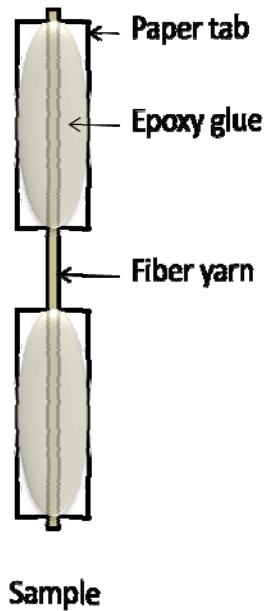


Figure 3. Schematic drawing of the specimen for SAXS measurements.

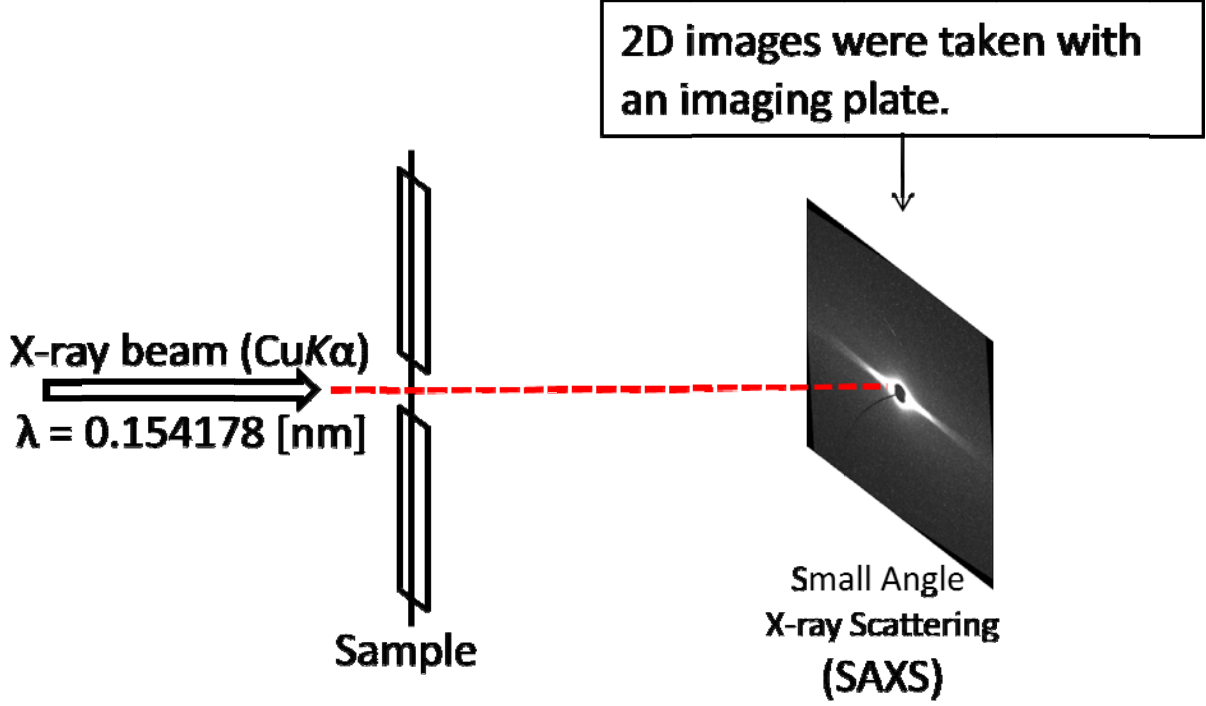


Figure 4. Beam arrangement for the SAXS measurements.

From the analytical method reported by Shioya and Takaku,¹⁰ the size parameters of the voids were calculated, (R_3 , S_3 , and l_3), and the segments, (l_2), from SAXS using the following equations:

$$\ln I(x) = -\frac{2\pi^2 R_3^2}{\lambda^2 L^2} x^2 + \ln S_3 + \ln \left(\frac{2\pi}{\lambda^2 L^2} \int_0^\infty I(x) x dx \right) \quad [1]$$

$$l_2 = \frac{\lambda L \int_0^\infty I(x) dx}{\pi \int_0^\infty I(x) x dx} \quad [2]$$

$$[I(x)]^{-2/3} = \left[\int_0^\infty I(x) x dx \right]^{-2/3} \times \left[\left(\frac{\lambda L}{2\pi l_3} \right)^{4/3} + \left(\frac{2\pi l_3}{\lambda L} \right)^{2/3} x^2 \right] \quad [3]$$

where $I(x)$ is the scattering intensity, x is the axis parallel to the scanning direction of SAXS, λ is the wavelength, and L is the SDD. $I(x)$ represents the total scattering intensity which is obtained by integrating in the direction parallel to the fiber axis the scattering intensity distribution at a distance x . R_3 is the average of the radius of gyration of the cross-section of a void. S_3 is the average cross-sectional area of a void, where the cross-section is perpendicular to the fiber axis. l_3 is the average of the thickness of a void, measured perpendicular to the fiber axis. The value l_2 , the average length of a segment defined by the contours of a void from an arbitrary straight line perpendicular to the fiber axis, was similarly calculated.

3. RESULTS

3.1 Mechanical Properties

As stated previously, significant decreases in mechanical properties of PBO fibers were found when they were subjected to folding. The results for PPTA, however, did not show a significant drop-off in mechanical properties. Table 1 shows that for PBO the tensile strength and strain-to-failure decreased as the sample progressed from an unfolded woven fabric extracted from SBA through 5 000 folds and 80 000 folds.

The tests were repeated for the PPTA fibers (see Table 2). In this case, very little change in mechanical properties caused by folding was observed. One possible reason for the difference in the mechanical response of PPTA and PBO fibers (described by Holmes et al.¹²) could be the relatively low compressive strength of the PBO fibers ($0.19 \text{ GPa} \pm 0.04 \text{ GPa}$) when compared to PPTA fibers (between $0.29 \text{ GPa} \pm 0.03 \text{ GPa}$ and $0.35 \text{ GPa} \pm 0.04 \text{ GPa}$).¹³ The \pm is the standard deviation and is taken as an estimate of the standard uncertainty. A second reason could be due to PPTA fibers having extensive hydrogen bonding between the amide linkages and PBO fibers having no hydrogen bonding.

Table 1: Data for PBO fibers tested using paper templates from Holmes et al.¹²

PBO Sample	Load, N	Strength, GPa	Modulus, GPa	Strain, %	Diameter, μm
Woven	0.450 ± 0.057	3.36 ± 0.37	143 ± 9.8	2.97 ± 0.39	13.1 ± 0.6
5k folds	0.384 ± 0.058	2.90 ± 0.42	146 ± 9.1	2.50 ± 0.45	13.0 ± 0.5
80k folds	0.279 ± 0.042	1.99 ± 0.30	136 ± 8.0	1.74 ± 0.32	13.3 ± 0.4

Table 2: Data for PPTA fibers tested using paper templates

PPTA Sample	Load, N	Strength, GPa	Modulus, GPa	Strain, %	Diameter, μm
Woven	0.411 ± 0.038	3.14 ± 0.31	84.7 ± 6.0	3.61 ± 0.35	12.9 ± 0.3
5k folds	0.404 ± 0.055	3.05 ± 0.41	82.9 ± 4.6	3.54 ± 0.45	13.0 ± 0.3
80k folds	0.415 ± 0.087	3.07 ± 0.43	85.0 ± 5.3	3.49 ± 0.43	13.0 ± 0.3

3.2 SAXS Measurements

As stated in the introduction, although the folded fibers were examined using SEM, no damage was observed on the surfaces of the fibers. This may be attributed to structural changes that occurred inside the fibers when they were folded. In an effort to observe the internal structure of the fibers by SEM, the fiber samples would have to be cut, which may damage the structure of interest to these observations. Moreover, these structures may be of “nano” dimensions that are difficult to observe with SEM. The same issue of potentially damaging the internal structure is also present when using TEM. Therefore, SAXS measurements were conducted to analyze these structures. Figure 5 shows SAXS images for the PPTA and PBO fibers. The streaks are scattering from the microvoids which are needle-like and oriented parallel to the fiber axis^{6,14}.

The parameters R_3 and S_3 were calculated from Equation 1 and the data in the Guinier plots (Figures 6) with the results shown in Figure 7, and l_3 and l_2 were calculated using Equations 2 and 3 with the results shown in Figure 8. In the case of PPTA, these values did not change when the fibers were folded. In the case of PBO, however, these values decreased when the fibers were folded.

Figure 5. SAXS images of the (a) PPTA unfolded, (b) PPTA folded 5,000 times, (c) PPTA folded 80 000 times, (d) PBO unfolded, (e) PBO folded 50 00 times, and (f) PBO folded 80 000 times. The scattering vector $Q = (4\pi/\lambda)\sin\theta$ with θ being the scattering angle.

Figure 6. Guinier plots of the (a) PPTA unfolded, (b) PPTA folded 5 000 times, (c) PPTA folded 80 000 times, (d) PBO unfolded, (e) PBO folded 5 000 times, and (f) PBO folded 80 000 times.

Figure 7. The (a) average of radius of gyration of void R_3 of PPTA, (b) average of cross section area of void S_3 of PPTA, (c) R_3 of PBO, and (d) S_3 of PBO. The error bars are taken as an estimate of the standard uncertainty.

From the analysis of the SAXS results, it was discovered that the average void and fibril sizes of PBO appeared to decrease when the fibers were folded. Therefore, one may surmise that the

fibrils in PBO were subdivided when the fibers were folded, or new voids were created thereby decreasing the average size of the fibrils. This subdivision creates new surfaces and defects inside the fiber. Therefore, this subdivision may influence not only mechanical properties but also hydrolytic degradation or other mechanisms that would lead to sources of failure. In the case of the PPTA fibers, no signs of structural changes were observed by the SAXS techniques. This stability of PPTA fiber might be attributed to the strong intermolecular hydrogen bonding known to be present in PPTA fibers, but lacking in PBO fibers.

Figure 8. The (a) average length of segment l_2 of PPTA, (b) average thickness of void l_3 of PPTA, (c) l_2 of PBO, and (d) l_3 of PBO. The error bars are taken as an estimate of the standard uncertainty.

4. CONCLUSIONS

Previous work in this group noted a significant drop-off of tensile strength and strain-to-failure in PBO fibers when subjected to repeated folding. Follow-up work on PPTA fibers showed a slight reduction in these mechanical properties. Results from X-ray analysis indicated that the void and fibril sizes of PBO were decreased when the fibers were folded. From these observations one may surmise that the fibrils in the filaments were subdivided when the fibers were folded. This subdivision makes new surfaces and defects inside the fiber. Thus, this subdivision may

influence not only mechanical properties but also hydrolytic degradation and other failure pathways, whereas for PPTA fibers, there were no signs of structural changes.

5. REFERENCES

1. Holmes, G. A., Rice, K., & Snyder, C. R. "Ballistic Fibers: A Review of the Thermal, Ultraviolet and Hydrolytic Stability of the Benzoxazole Ring Structure." *Journal of Materials Science* 41 (2006): 4105-4116.
2. Holmes, G. A., Kim, J. H., McDonough, W. G., Riley, M. A., & Rice, K. D. "A Detailed Investigation of The Mechanical Properties of Polybenzoxazole Fibers Within Soft Body Armor." *Journal of Materials Science* 44 (2009): 3619-3625.
3. Park, E. S., Sieber, J., Guttman, C. M., Rice, K. D., Flynn, K. M., Watson, S., & Holmes, G. A. "Methodology for Detecting Residual Phosphoric Acid in Polybenzoxazole Fibers." *Analytical Chemistry* 81 (2009): 9607-9617.
4. Chin, J., Byrd, E., Forster, A. L., Gu, X., Nguyen, T., Rossiter, W., Scierka, S., Sung, L., Stutzman, P., Sieber, J., & Rice, K. "Chemical and Physical Characterization of Poly(p-Phenylene Benzobisoxazole) Fibers Used in Body Armor." *NISTIR 7237*. National Institute of Standards and Technology, Gaithersburg, MD (2005).
5. Clements, L. L. "Organic Fibers". *Handbook of Composites*. Peters, S. T. ed. London: Chapman & Hall, 1998. 202-241.
6. Kitagawa, T., Murase, H., & Yabuki, K. "Morphological Study on Poly-p-phenylenylenebenzobisoxazole (PBO) Fiber." *Journal of Polymer Science: Part B: Polymer Physics* 36 (1998): 39-48.
7. Holmes, G. A., Kim, J. H., Ho, D. L., & McDonough, W. G. "The Role of Folding in the Degradation of Ballistic Fibers." *Polymer Composites* (2009):
8. Kim, J. H., Brandenburg, N., McDonough, W., Blair, W., & Holmes, G. A. "A Device for Mechanically Folding Yarns and Woven Fabrics of Ballistic fibers." *Journal of Applied Mechanics* 75 (2008):
9. Chau, C. C., Blackson, J., & Im, J. "Kink bands and shear deformation in polybenzobisoxazole fibres." *Polymer* 36 (1995): 2511-2516.
10. Shioya, M., Takaku, A. "Characterization of microvoids in carbon fibers by absolute small-angle x-ray measurements on a fiber bundle." *Journal of Applied Physics* 58 (1985): 4074-4082.
11. Kim, J. H., McDonough, W., Blair, W., & Holmes, G. A. "The Modified-Single Fiber Test: A Methodology for Monitoring Ballistic Performance." *Journal of Applied Polymer Science* (2008): 876-886.
12. Holmes, G. A., Park, E. S., Sieber, J., Kim, J. H., McDonough, W., Kobayashi, H., & Rice, K. "A Critical Look at Damage Mechanisms in Ballistic Fibers". *Personal Armor Systems Symposium*. Quebec, Canada: 2010.
13. Leal, A. A., Deitzel, J. M., & Gillespie Jr., J. W. "Assessment of compressive properties of high performance organic fibers." *Composites Science and Technology* 67 (2007): 2786-2794.

14. Dobb, M. G., Johnson, D. J., Majeed, A., & Saville, B. P. "Microvoids in aramid-type fibrous polymers." *Polymer* 20 (1979): 1284-1288.